

## Observation of Surface Plasmons and Measurement of the Optical Constants for Sodium and Potassium†

Richard E. Palmer\* and Stephen E. Schnatterly‡

*Joseph Henry Laboratories of Physics, Princeton University, Princeton, New Jersey 08540*

(Received 6 May 1971)

The optical constants of sodium and potassium from 1.75 to 4.5 eV are measured using a highly sensitive ellipsometric technique developed by Schnatterly and Jasperson. Measurements are made on the vacuum interface of films vacuum deposited at 77°K. Surface plasmons are readily observed, and their decay with time and temperature gives estimates of the activation energy and lattice-vibrational frequency associated with the annealing properties of the metallic surface. The plasma frequency and electronic "optical" mass (at visible and near-ultraviolet frequencies) are calculated from the real part of the dielectric constant and found to be  $3.8 \pm 0.1$  eV ( $5.4 \pm 0.2$  eV) and  $(1.08 \pm 0.02)m_e$  [ $(1.00 \pm 0.02)m_e$ ] for potassium (sodium). The energy-loss function for potassium is given, and the room-temperature optical constants measured for sodium and potassium are tabulated for future use.

### I. INTRODUCTION

Sodium and potassium are very good approximations to a nearly-free-electron metal, and therefore, they have been the object of considerable theoretical interest. A study of the optical properties of these metals can yield information about the plasma frequency and the optical effective mass of the electrons.<sup>1</sup> The conductivity at frequencies below the onset of interband transitions provides a measure of the mean electron-collision time, and the conductivity in the interband region gives information about the Fourier components of the pseudopotential.<sup>2-5</sup>

Early experimental measurements of the optical constants of the alkali metals were done by Ives and Briggs<sup>6,7</sup> and by Duncan and Duncan.<sup>8</sup> Later work was done by Hodgson,<sup>9,10</sup> by Mayer and co-workers,<sup>11,12</sup> by Althoff and Hertz,<sup>13</sup> and by Sutherland and co-workers.<sup>14,15</sup> The most recent work has been performed by Smith.<sup>16</sup> Unfortunately, the experimental difficulties involved in measuring the optical constants of the alkali metals are numerous, and the results have not been very consistent.

With this in mind and with the advent of new ellipsometric techniques, the present experiment was performed. In Sec. II of this paper, a new ellipsometric technique developed by Schnatterly and Jasperson to measure the optical constants of high-reflectivity metals is briefly discussed. This method is differential and extremely sensitive to small changes in the reflectivity. It is possible to scan continuously in wavelength with this technique. The difficulties and procedures involved in preparing highly specular sodium and potassium films are also discussed in this section. Section III contains experimental results for the real part of the dielectric constant, which provides a measure of the plasma frequency and of the optical effective mass

of the electrons. Section IV is a discussion of the observation of optically excited collective (plasmon) modes, in particular, surface plasmons, which may prove to be a useful tool in studying the roughness and annealing properties of the metal surface. Section V presents the conductivity for sodium and potassium in the interband region. However, as in past experiments, the question of how to subtract out the Drude tail remains a problem, since it does not behave as theoretically predicted. Section VI contains a calculation of the energy-loss function for potassium, which shows a sharply peaked absorption at the plasma frequency. The room-temperature optical constants of sodium and potassium are tabulated in Sec. VII.

### II. EXPERIMENTAL TECHNIQUE

#### A. Ellipsometry

A basic technique for measuring the optical constants of high-reflectivity metals is ellipsometry, which measures the relative magnitude and phase shift of the reflectivity for light whose polarization is perpendicular to and for light whose polarization is parallel to the plane of incidence for non-normal incidence. The ellipsometric method used in this experiment was developed by Jasperson and Schnatterly,<sup>17</sup> and later improved by Callender.<sup>18</sup> It has the advantage over other methods in that the optical constants can be scanned continuously in wavelength, thereby allowing a run to be done in a short period of time and bringing out small details in structure that might be missed in a point-by-point measurement. Since the technique has been described elsewhere,<sup>17</sup> it will be discussed only briefly below.

For light that strikes a metal interface at non-normal incidence, the reflectivity amplitude for light polarized parallel ( $p$  polarization) to the plane of incidence differs from the reflectivity amplitude

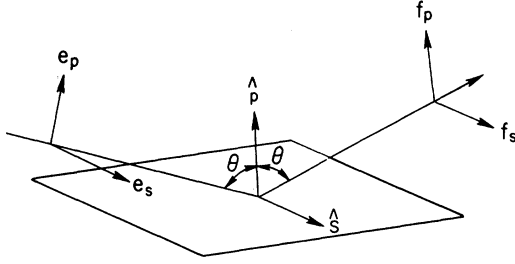


FIG. 1. Reflection of light from a surface at non-normal incidence. Ellipsometry measures the relative magnitude and phase of the reflectivity amplitudes for light polarized parallel to and perpendicular to the plane of incidence.

for light polarized perpendicular (*s* polarization) to the plane of incidence (see Fig. 1). The two reflectivity amplitudes  $f$  are given by Fresnel's equations

$$f_p \equiv r_p e^{i\delta_p} = \tan(\theta - \tilde{\psi}) / \tan(\theta + \tilde{\psi}), \quad (1)$$

$$f_s \equiv r_s e^{i\delta_s} = -\sin(\theta - \tilde{\psi}) / \sin(\theta + \tilde{\psi}). \quad (2)$$

Here  $r_p$  ( $r_s$ ) is the magnitude and  $\delta_p$  ( $\delta_s$ ) is the phase shift of the reflectivity amplitude for light polarized parallel (perpendicular) to the plane of incidence.  $\theta$  is the angle of incidence (it is equal to  $45^\circ$  in this experiment), and  $\tilde{\psi}$  is the complex angle of refraction, which is determined by Snell's law

$$\sin\theta = (\tilde{\epsilon})^{1/2} \sin\tilde{\psi}. \quad (3)$$

$\tilde{\epsilon}$  is defined as the complex dielectric constant of the metal and is given by

$$\tilde{\epsilon}(\omega) \equiv \epsilon_1 + i\epsilon_2 = \epsilon + 4\pi i\sigma(\omega)/\omega, \quad (4)$$

where  $\sigma(\omega)$  is the conductivity of the metal.

The experimental quantities measured are

$$N \equiv (r_s^2 - r_p^2) / (r_s^2 + r_p^2), \quad (5a)$$

$$C \equiv \cos\Delta = \cos(\delta_s - \delta_p), \quad (5b)$$

$$S \equiv \sin\Delta = \sin(\delta_s - \delta_p). \quad (5c)$$

Either  $\cos\Delta$  or  $\sin\Delta$  can be measured alone if the quadrant in which  $\Delta$  lies is known. Measuring both gives a consistency check. The dielectric constant  $\tilde{\epsilon}$  of the metal can be calculated from  $N$ ,  $S$ , and  $C$ :

$$\epsilon_1 = \sin^2\theta + \sin^2\theta \tan^2\theta \frac{N^2 - (1 - N^2)S^2}{[1 + C(1 - N^2)^{1/2}]^2}, \quad (6)$$

$$\epsilon_2 = 2 \sin^2\theta \tan^2\theta \frac{NS(1 - N^2)^{1/2}}{[1 + C(1 - N^2)^{1/2}]^2}. \quad (7)$$

The absorption, conductivity, reflectivity, etc., can be calculated once  $\tilde{\epsilon}$  is known.

This analysis is valid for an isotropic nonmagnetic material, for which  $\tilde{\epsilon}$  is a scalar and describes the optical properties completely. The alkali metals

fall into this class. The films were made thick enough so that reflections from the metal-substrate interface did not have to be considered.

Local response is another assumption and must be carefully considered. The alkali metals are in the anomalous skin effect region for the wavelengths of light used in most optical experiments. The characteristic electron-collision frequency must now include a surface-scattering term  $1/\tau_s$ , so that the collision frequency becomes<sup>9,16,19,20</sup>

$$1/\tau = 1/\tau_b + 1/\tau_s, \quad (8)$$

where  $1/\tau_b$  is the electron-collision frequency of the bulk metal. Thus,  $\tilde{\epsilon}$  is redefined to include surface collisions. Theoretical interpretations of measurements of  $\tilde{\epsilon}$  must consider this point.

### B. Sample Preparation

The metal films were prepared inside an ultra-high-vacuum chamber which could attain a base pressure of  $5 \times 10^{-10}$  Torr. The pump was a Varian 20-liter/sec Vac-Ion pump. Two fused-spectrosil-quartz windows allowed the light to strike and leave the sample at  $45^\circ$ . One of the prepared ampoules<sup>21</sup> was placed in the oven, as in Fig. 2. The collector was used for a photoemission experiment, but it also acted as a mask and as a means to break open the ampoule. The collector was normally in the lower position.

The oven consisted of a  $2\frac{1}{2}$ -in.-long by  $\frac{5}{16}$ -in.-i.d. quartz tube surrounded by a cylinder of 0.001-in.-thick tantalum foil. Electrodes were attached to the two ends of the tantalum cylinder and high current feedthroughs allowed one to apply large currents through the cylinder. A dc magnet power supply was used as a current source.

Preparation of the films proceeded as follows: The vacuum chamber was sealed and pumped down. It was then baked at  $250$ – $300^\circ\text{C}$  for about 2 days until the base pressure was reached. After the sys-

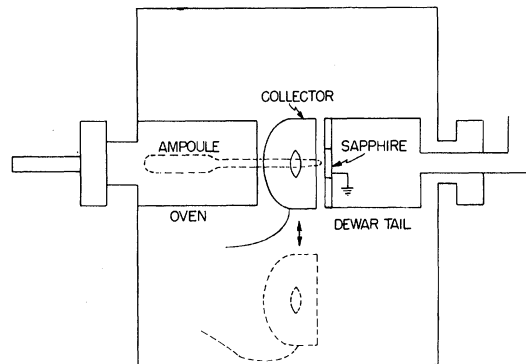


FIG. 2. Schematic of vacuum chamber. The collector can be raised or lowered and acts as a mask and as a means to open the ampoule.

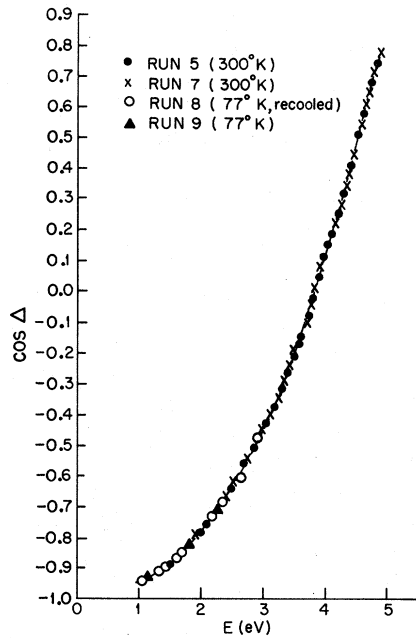


FIG. 3.  $\cos\Delta$  for potassium.  $\Delta$  is the relative phase shift upon reflection for light polarized perpendicular and parallel to the plane of incidence.

tem had cooled, the collector was raised to break off the tip of the ampoule and to shield the substrate from the oven. The evaporation of metal was detected with a quartz crystal oscillator thickness monitor (Sloan DTM-3). The oven and ampoule were outgassed by applying a current just below that which would cause any change in the thickness monitor. This corresponded to a current of 15 and 18 A for sodium and potassium, respectively. The voltage was roughly 1 V. The outgassing was continued until the pressure fell to the  $10^{-10}$ -Torr scale (typically 1 day or less) and then was stopped.

The evaporations were performed while the substrate was at 77°K. At first, glass or quartz substrates were used, but the sodium films were somewhat grainy, and diffuse nonspecular scattering was visible. We speculated that the thermal conductivity of the quartz was too low to provide sufficient cooling of the front side of the substrate during evaporation. Sapphire substrates were therefore substituted for the quartz, since the thermal conductivity of sapphire is comparable to that of copper at 77°K. When the sapphire substrates were used, the sodium films (as well as the already good potassium films) were perfectly specular (to the eye), with no granularity and no nonspecular scattering. Even with our high intensity xenon lamp (450 W), no light could be seen coming from the films, unless the eye were directly in the specular beam.

After the substrate was cooled to 77°K, the cur-

rent in the oven was turned up to 25 A (33 A), at which point the thickness monitor would detect evaporation of sodium (potassium). The pressure rose to the  $10^{-8}$  Torr scale and was presumably due to the metal vapor. The photoemission collector was then lowered to expose the substrate, and 2000 Å of metal was deposited in 1–2 min. If the metal were deposited at a much slower rate, the films tended to be grainy. Other authors<sup>22,23</sup> have also noticed that rapid evaporation rates improve the specularity of the films. Films much thicker than 4000–5000 Å had difficulty adhering smoothly to the substrate, and films thinner than 1000 Å would allow the light to penetrate to the substrate interface. A thickness of 2000 Å was chosen as a compromise between the two extremes.

When 2000 Å had been deposited, the collector was raised to shield the film. The oven was turned off and cooled in a few minutes. The collector was then lowered again, and the experiment was performed.

### III. REAL PART OF DIELECTRIC CONSTANT

For a nearly-free-electron metal, the real part of the dielectric constant is given by<sup>24</sup>

$$\epsilon_1 = 1 - \frac{\omega_p^2}{\omega^2} - \frac{4\pi e^2}{m} \sum'_{\mu} \frac{F_{0\mu}}{\omega^2 - \omega_{\mu 0}^2}, \quad (9)$$

where the prime on the summation indicates  $\mu = 0$  to be omitted from sum. The third term is the contribution from interband transitions. Here  $F_{0\mu}$  is the oscillator strength of the conduction band to  $\mu$ th band transition and  $\omega_{\mu 0} = \omega_{\mu} - \omega_0$ . The plasma frequency squared is  $4\pi n e^2 / m^*$ , and if  $n$  is assumed to be one electron per atom,  $\omega_p^2$  gives the optical effective mass  $m^*$  of the electrons. In the visible and the near-ultraviolet region the interband contribution should have a term proportional to  $\omega^{-2}$ . This term can be absorbed into the second term on the right-hand side of Eq. (9) and can be regarded as a correction to the optical effective mass at visible and near-ultraviolet frequencies.<sup>1</sup> The interpretation of the optical mass in the interband region is presently somewhat confused,<sup>16</sup> and in this paper it will be taken to be only the experimentally measured slope of  $\epsilon_1$  vs  $\omega^{-2}$ .

For high-reflectivity metals  $N = (r_s^2 - r_p^2) / (r_s^2 + r_p^2)$  is typically about 0.01 in the optical region, and thus  $\epsilon_1$  depends on  $\sin\Delta$  or  $\cos\Delta$  [see Eq. (6)].

Experimental results for  $\cos\Delta$  ( $\sin\Delta$ ) for potassium (sodium) are shown in Fig. 3 (4). The choice between measuring  $\sin\Delta$  or  $\cos\Delta$  is determined by the magnitude of  $\Delta$ ; if  $\Delta$  is small (large), then  $\sin\Delta$  ( $\cos\Delta$ ) is the more sensitive quantity. It was observed that  $\sin\Delta$  or  $\cos\Delta$  was extremely repeatable, not only from sample to sample, but also for the same sample after it was annealed at room temperature. However, the absorption would vary great-

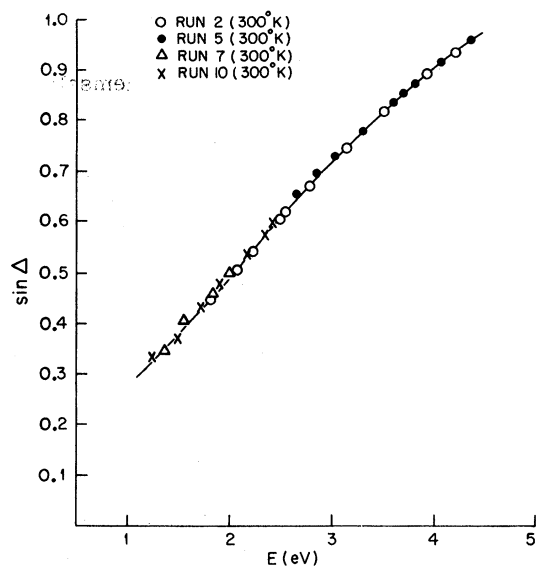


FIG. 4.  $\sin\Delta$  for sodium.  $\Delta$  is the relative phase shift upon reflection for light polarized perpendicular and parallel to the plane of incidence.

ly. This is because  $\sin\Delta$  or  $\cos\Delta$  is determined by  $\epsilon_1$ , which depends primarily on the electron density (the effective mass is always close to  $m_e$ ). Furthermore, the electron density  $n$  depends only weakly on the microstructure (e.g., amorphous, single crystalline, polycrystalline, etc.) and on

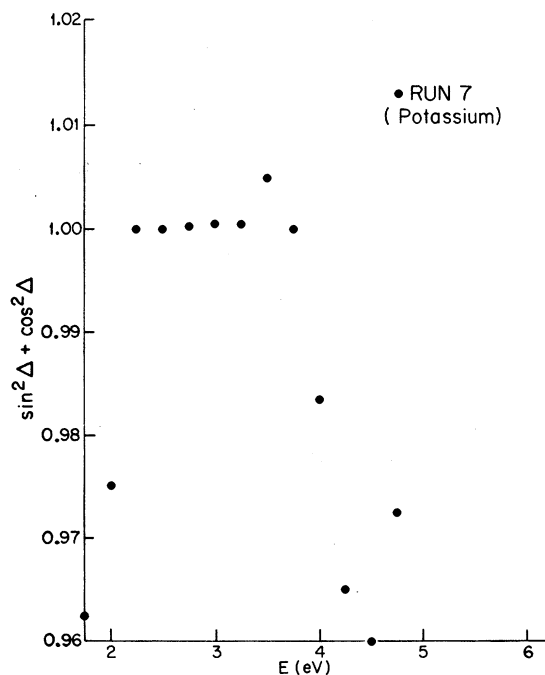


FIG. 5.  $\sin^2\Delta + \cos^2\Delta$  for one run of potassium. Its deviation from unity determines the wavelength range of the experiment.

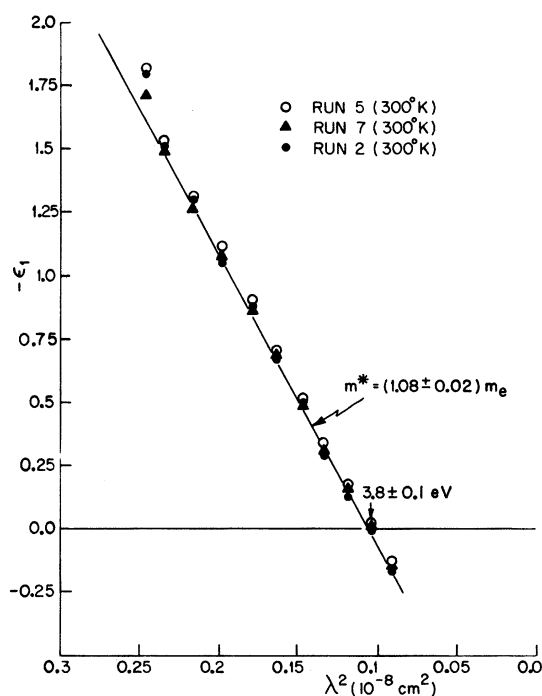


FIG. 6.  $\epsilon_1$  vs  $\lambda^2$  for potassium. The slope gives  $m^*$  and the  $x$  intercept gives the plasma frequency.

the surface structure of the film, which cannot be said for the absorption.

Occasionally, both  $\cos\Delta$  and  $\sin\Delta$  were measured to check for consistency. Figure 5 is an example of one such run for potassium. The deviation of  $\sin^2\Delta + \cos^2\Delta$  from unity at the long-wavelength end was due to the failing infrared response of the photomultiplier tube, which had an S-20 photoresponse. Deviations in the ultraviolet were due to scattered light in the monochromator. These limits determined the effective wavelength range of the experiment. For some measurements an infrared photomultiplier tube (S-1 photoresponse) was used to extend the measurements down to 1.1 eV.

Results from measurements of  $\cos\Delta$  or  $\sin\Delta$  and of  $N$  (which are discussed in Sec. IV) were used to calculate  $\epsilon_1$ . Figures 6 and 7 show  $\epsilon_1$  plotted as a function of  $\lambda^2$  (or  $\omega^{-2}$ ) for potassium and sodium, respectively. The straight-line fit is quite good and repeatable over the optical region. At longer wavelengths the slope of  $\epsilon_1$  vs  $\lambda^2$  is smaller, because the interband contribution is weaker.<sup>16</sup>

The  $x$  intercept gives the plasma frequency.  $\omega_p$  for potassium was found to be  $3.8 \pm 0.1$  eV, which was in good agreement with Smith<sup>16</sup> and with Sutherland *et al.*<sup>15</sup> The plasma frequency for sodium was found to be  $5.4 \pm 0.2$  eV by extrapolating  $\epsilon_1$  to the  $x$  axis. Very slight positive curvature was present at the high-energy end of our data, and the slightly higher value for  $\omega_p$  obtained by Smith<sup>16</sup> and by

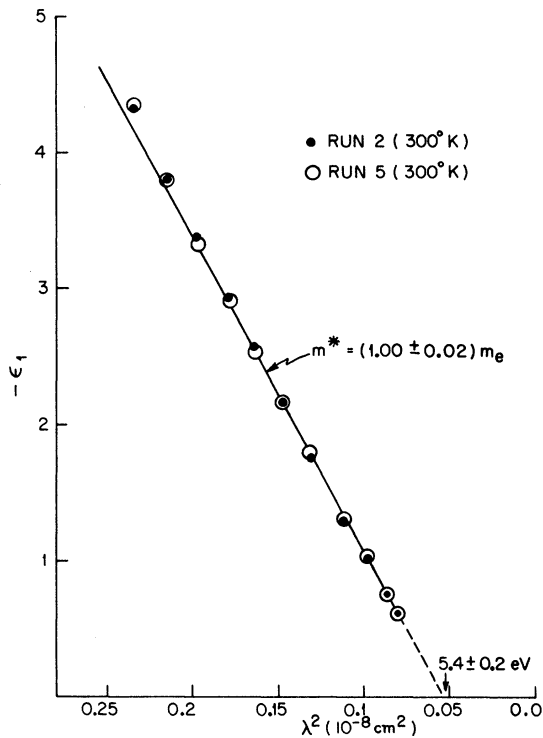


FIG. 7.  $\epsilon_1$  vs  $\lambda^2$  for sodium. The slope gives  $m^*$  and the  $x$  intercept gives the plasma frequency.

Sutherland *et al.*<sup>14</sup> is probably more reliable. However, our results are by no means in conflict with theirs. The value of  $\epsilon_1$  for  $\lambda=0$  was extrapolated and found to be  $1.25 \pm 0.05$  for both metals. This is not the true value of  $\epsilon_1$  at  $\lambda=0$ , because the contribution from interband transitions will be different at higher energies from what it is in the optical region.

The slope of  $\epsilon_1$  vs  $\lambda^2$  gives the optical mass at visible and near-ultraviolet frequencies. Table I compares the results of this experiment with those of other authors. Except for Mayer *et al.*, the agreement is very good.

#### IV. OBSERVATION OF SURFACE PLASMONS

The existence of surface plasmons was predicted by Ritchie<sup>25</sup> and later extended by Ferrell<sup>26</sup> and by Stern and Ferrell.<sup>27</sup> Experimental evidence for the existence of surface plasmons was found by Powell and Swan<sup>28</sup> in the energy-loss spectra of fast electrons incident on Al and Mg. Their findings were supported by the work of Boersch and co-workers<sup>29-31</sup> and of Arakawa and co-workers.<sup>32,33</sup> More recently, direct optical excitation of surface plasmons has been observed by Schnatterly and Jaspersen,<sup>34</sup> and by Hunderi and Beaglehole.<sup>35-38</sup> Their results verified the earlier work of Teng and Stern,<sup>39</sup> which indicated that surface roughness is

the dominant mechanism which couples the surface plasmon to electromagnetic radiation.

Surface plasmons should manifest themselves in an optical experiment as an additional absorption peak at a frequency such that  $\epsilon(\omega) = -\epsilon_0$ , where  $\epsilon_0$  is the dielectric constant of the medium present at the metal surface; for a vacuum interface  $\epsilon_0=1$ . If the dielectric constant of the metal is given as in Eq. (32) of Ref. 26, then the surface plasmon peak should occur at  $\omega = \omega_p(2)^{-1/2}$  for  $\epsilon_0=1$ , and it should have a width

$$1/\tau_d = \epsilon_2 \omega^3 / \omega_p^2. \quad (10)$$

As was mentioned in Sec. III,  $\cos\Delta$  or  $\sin\Delta$  is a quite repeatable quantity, even if the absorption differs widely from sample to sample. Thus, as can be seen in Eq. (7), structure in  $\epsilon_2(\omega)$  will appear as a change in  $N$ , which is proportional to  $\epsilon_2$ .

In Figs. 8 and 9 representative measurements of  $N$  for potassium and sodium are shown. On a single sample three runs were performed. The first was done initially right after the sample was prepared at 77°K. The sample was then warmed to 300°K and the run repeated. Finally, the sample was recooled to 77°K for a third run.

An absorption peak appeared at 2.8 and 4.0 eV for potassium and sodium, respectively, in the initial run at 77°K. When the sample was warmed to 300°K, the peak disappeared, and it did not reappear when the film was recooled to 77°K. Occasionally in sodium the peak would reappear very weakly when the sample was recooled. We attribute this to slight wrinkling of the film due to thermal contraction. However, the new peak was always much smaller than the original peak.

From Figs. 6 and 7 it can be seen that  $\epsilon_1 = -1$  at 2.8 and 4.0 eV for potassium and sodium, respectively. The plasma frequency divided by the energy of the resonance appearing in  $N$  is 1.36 (1.35) for potassium (sodium), showing that if indeed this resonance is a surface plasmon, then Eq. (32) of Ref. 26, which predicts a ratio of 1.41, adequately describes the dielectric constant  $\epsilon(\omega)$  of these metals. The reason that the observed ratio is not

TABLE I. Values for the optical mass for Na and K in the visible and near-ultraviolet region.

	Na	K
This experiment	$1.00m_e$	$1.08m_e$
Smith	1.07	1.06
Mayer and co-workers	1.17	1.00
Hodgson	1.00	...
Cohen <sup>a</sup>	1.01	1.08

<sup>a</sup>Analysis of Ives and Briggs's data.

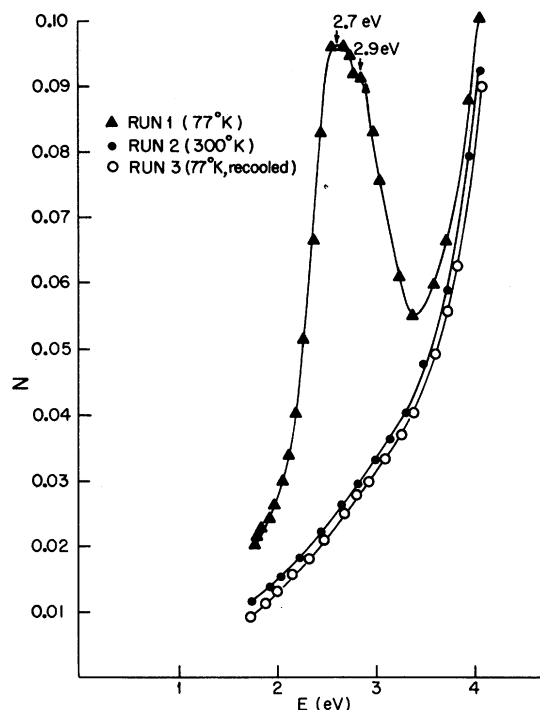


FIG. 8.  $N = (r_s^2 - r_p^2) / (r_s^2 + r_p^2)$  for potassium.  $N$  is proportional to  $\epsilon_2$ . Three runs were performed on each sample: one at 77°K, one at 300°K, and one again at 77°K. The structure near 2.8 eV is due to surface plasmons.

1.41 is probably that the interband contribution to  $\epsilon_1$  (see Eq. 9) is different at the bulk plasmon frequency from the contribution at the surface plasmon frequency.

If the resonance were due to an intrinsic property of the metal, e.g., phonons, impurities, etc., we would expect the peak to reappear reversibly when the film was recooled. If the resonance depended on surface roughness, however, annealing of the film at warm temperatures would remove the peak for good. Surface plasmons do depend on surface roughness to couple to light, and this identifies the resonance as a surface plasmon.

The peaks were observed to have the structure of a double peak, the separation of which was 0.2 eV for both metals. The relative heights of the two peaks were fairly close, although on different runs the high-energy peak could be slightly higher, lower, or equal to the low-energy peak. Thin films are expected to have plasmons with two peaks,<sup>26</sup> since the plasmons at each surface are degenerate and will couple to each other to form an energy splitting. However, theory does not adequately explain the behavior of the peaks seen in this experiment, since both interfaces of the metal do not have  $\epsilon_0 = 1$ . The explanation for the double-peak structure seen is not fully determined at this time.

The width of the surface plasmon peak is much greater than that predicted by Eq. (10). Presumably this is because the surface plasmons are localized at the surface, where surface collisions greatly increase the electron-collision rate, thereby increasing the damping of the surface plasmon mode. Equation (10) applies to bulk properties alone, and in Sec. VI it will be shown that it works very well in the case of the bulk plasmon lifetime.

Fedders<sup>40</sup> has derived the change in the reflectivity for normal incidence produced when surface plasmons couple through surface roughness. The normal incidence reflectivity change was calculated and found to be 0.2 for run 2 in potassium and 0.02 for run 8 in sodium. These are representative values. A knowledge of the Fourier components of the surface roughness is required, but for the sake of simplicity we will assume only one Fourier component, with a wave vector of  $10^6 \text{ cm}^{-1}$ . This value was obtained by Jasperson and Schnatterly in their work on Ag and was obtained by measuring the downshifting in energy of the surface plasmon peak when a thin overcoat of  $\text{MgF}_2$  was applied. Such a procedure was not possible in the present experiment.

For one Fourier component  $k$ , the change in the normal incidence reflectivity predicted by Fedders<sup>40</sup> is

$$\Delta R = 2\pi a^2 k k_0, \quad (11)$$

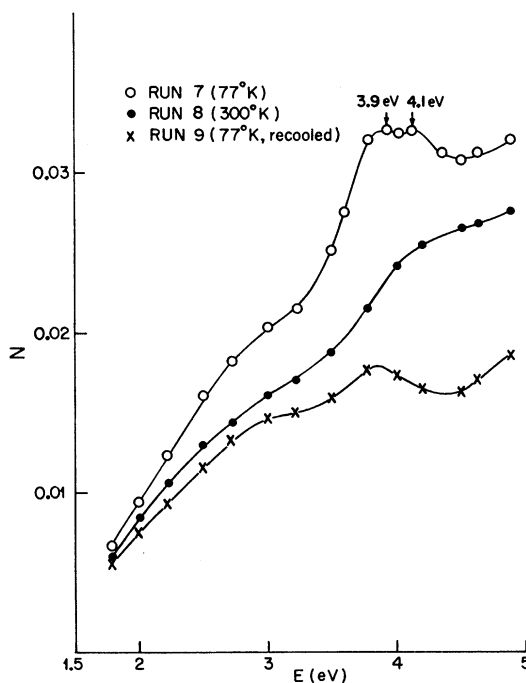


FIG. 9.  $N = (r_s^2 - r_p^2) / (r_s^2 + r_p^2)$  for sodium.  $N$  is proportional to  $\epsilon_2$ . Three runs were performed on each sample: one at 77°K, one at 300°K, and one again at 77°K. The structure near 4.0 eV is due to surface plasmons.

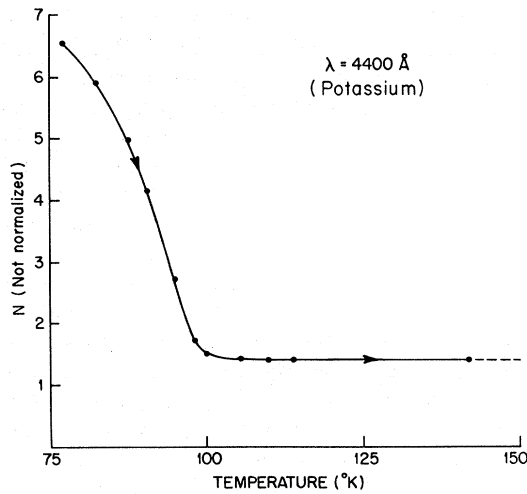


FIG. 10. Decay of a surface plasmon peak in potassium as the film is warmed from 77 to 300°K (in about 30 min). Subsequent recooling does not make the peak reappear.

where  $k_0$  is the magnitude of the wave vector of the light and  $a$  is the rms roughness. For  $\Delta R = 0.2$ ,  $k = 10^6 \text{ cm}^{-1}$ , and  $k_0 = \omega_p / c\sqrt{2} = 1.4 \times 10^5 \text{ cm}^{-1}$  the rms roughness  $a$  is 50 Å, which is a reasonable result. However, the roughness calculated in this manner depends on the choice of Fourier components used.

Since surface plasmons couple to light through surface roughness, they should provide information about the structure of the surface and its annealing properties. Figure 10 is an example of the decrease in the surface plasmon peak as a potassium film is warmed from 77 to 300°K. The film took about  $\frac{1}{2}$  h to reach room temperature. The shape of the curve depends on the rate of temperature increase, because the film is annealing even if the temperature is held fixed. At low temperature the peak falls slowly and as the temperature increases, the decay rate increases rapidly. At 100°K the decay rate is so rapid that the plasmon has disappeared. Subsequent recooling does not have any effect.

If the distribution of the surface is assumed to be  $\sin(kx)e^{-t/\tau}$ , where  $k$  is a characteristic wave vector and  $\tau$  a characteristic decay time, then self-diffusion data for potassium<sup>41</sup> should predict  $\tau$  for a given choice of  $k$ .  $\tau$  was found to be essentially infinite at 77°K for any reasonable choice of  $k$  because of the exponential factor  $e^{-Q/kT}$ , where  $Q$  is the activation energy.

However, the plasmon was found, in fact, to decay at 77°K with a  $\tau$  of roughly  $10^4$  sec. (This was measured by scanning the peak, waiting a few minutes, and then rescanning the peak to see if it had decreased.) Hence the annealing mechanism cannot be self-diffusion alone at 77°K. This is to be expected, because the presence of the surface de-

stroys the random-walk nature of the relaxation, and indeed surface-tension effects must be the dominant mechanisms at low temperature. If we assume that the atoms migrate by squeezing through vacancies (as in self-diffusion), then the jump probability  $e^{-Q/kT}$  should remain roughly the same.  $Q$  is the energy necessary to squeeze through the vacancy. The value of  $Q$  determined by self-diffusion data for potassium is  $Q = 0.42 \text{ eV}$  per atom. The frequency factor  $D_0$  should now reflect surface-tension effects and not random-walk self-diffusion, at least at 77°K.

If we assume that

$$N = N(0)e^{-t/\tau}, \quad \tau = \tau_0 e^{Q/kT}, \quad (12)$$

then the graph of  $N$  vs  $T$  in Fig. 10 provides a measure of  $Q$ .  $\tau$  is  $\sim 10^4$  sec at 77°K. By equating the slope at 77°K divided by the value of  $N$  at 77°K to

$$\frac{dN}{dT} / N = -\frac{tQ}{kT^2},$$

and taking  $t = 300$  sec, we find  $Q \approx 0.25 \text{ eV}$  (5.8 kcal/mole), in good order-of-magnitude agreement with the value obtained by self-diffusion data. (Large uncertainties in the value of  $t$  chosen could explain the factor-of-2 difference.) Thus, we have  $1/\tau_0 \approx 10^{13} \text{ sec}^{-1}$ , which is close to previously calculated values of atomic lattice-vibrational frequencies for the alkali metals.<sup>42</sup>

A small peak in  $\epsilon_2$  ( $\Delta\epsilon_2 \approx 0.007$ ) was observed at the bulk plasma frequency in potassium. It remained even after the films were annealed at room temperature, and we attribute it to the optical excitation of bulk plasmons in thin films described by Ferrel and Stern,<sup>43</sup> or to enhancement of  $\epsilon_2$  near the plasma frequency arising from electron-electron interactions, as discussed by Hopfield.<sup>44</sup>

## V. INTERBAND TRANSITIONS

The strength of the interband transitions can yield information about the pseudopotential of the metal, since the matrix elements are the Fourier components of the pseudopotential for the reciprocal lattice vectors associated with the final state. At optical frequencies, the only important transition is to the (110) band, and, in theory, the optical constants can determine  $V_{110}$ .

However, in order to measure the interband transition strength, the Drude or intraband contribution must be subtracted. As in past experiments, the behavior of the Drude tail does not follow the expected  $\omega^{-2}$  dependence, so that the validity of calculating the interband transition strength is questionable.

Anomalous behavior of the Drude tail has been seen many times before, not only in the alkali metals,<sup>16,45</sup> but also in Cu, Ag,<sup>46</sup> and Al.<sup>47</sup> In their papers, Ehrenreich and Phillip attribute the break-

down in the simple Drude theory to the ability of interband transitions to affect the optical constants below the interband threshold through the Kramers-Kronig relations between  $\epsilon_1$  and  $\epsilon_2$ . Bennett and Bennett<sup>48</sup> have shown, however, that this effect would be too small to explain the observed results. The anomalous skin effect also fails to justify the experimental data.<sup>16</sup>

The fact that experimental data fit the Drude theory better as sample preparation techniques improve<sup>48</sup> suggests that the decrease in the reflectivity due to scattering by surface roughness<sup>49</sup> may explain the anomalous behavior of the Drude tail. This would result in an apparent increase in the conductivity, until the intrinsic (smooth surface) reflectivity  $R_0$  begins to fall as the light frequency increases into the interband region. [The extra contribution to the conductivity due to surface roughness effects has the coefficient  $R_0/(1 - R_0)$ , and is important only when  $R_0$  is extremely close to unity.<sup>50</sup>]

Because of the failure of the simple Drude theory, only qualitative details of the contribution to the conductivity from interband transitions are described below.

#### A. Potassium

The most recent measurements of the optical constants of sodium and potassium have been made by Smith<sup>16</sup> and the results of the present experiment will be compared to his. The conductivity for potassium in the interband region is presented in Fig. 11. The curve peaks in the vicinity of 2 eV and then slowly decreases as the energy increases. Agreement of our results with Smith's near 2 eV is good, but the conductivity in our case falls off more slowly with increasing energy. This may be due to a higher electron-electron collision time, so that the contribution to the conductivity proportional to  $\omega^2$  proposed by Gurzhi<sup>51</sup> would be greater. This is not likely however, because Umklapp processes are not strong in the alkali metals (the periodic potential is very weak) and, therefore, electron-electron collisions do not contribute very much to the conductivity. It may be due to increased coupling to bulk plasmon modes, but the discrepancy between our data and Smith's becomes significant well below the plasma frequency.

The most plausible explanation is the difference in surface conditions in the two experiments. Surface roughness seems to be an important factor. Furthermore, the presence of a dielectric (quartz) at the reflecting interface, as in other experiments, qualitatively changes the shape of the conductivity (see discussion of sodium below). Kliewer and Fuchs<sup>52</sup> have proposed that the conductivity would be enhanced for light polarized parallel to the plane of incidence, because the component normal to the

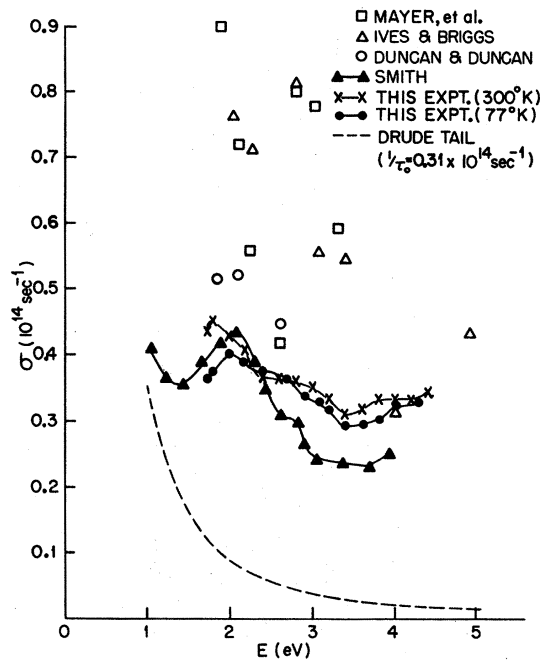


FIG. 11. Optical conductivity of potassium compared with previous experiments.

surface would create a polarization charge distribution at the surface which would produce large electric fields. The electrons would respond to these fields and enhance the absorption (and thus the conductivity) at and below the plasma frequency. The presence of a dielectric at the surface would depolarize these fields and reduce the absorption. This explanation works in the case of potassium, where the conductivity is higher for a free surface than for a quartz-metal interface (Smith), but we shall see that it fails in the case of sodium. Thus, further work must be done to establish definitely the causes for the discrepancies in the data. Present experimental sensitivities are too good to explain these differences. It can be seen, however, that agreement between the present experiment and Smith's is much better than that of earlier experiments.

#### B. Sodium

The results for sodium are quite different from those for potassium. As can be seen in Fig. 12, there are two qualitative differences between the conductivity measured by Smith and by the present experiment. The Drude tail below the interband threshold (2 eV) is roughly twice as large for this experiment as for Smith's. Also, the magnitude of the interband transition strength is much smaller than that measured by Smith. Since the Drude tail does not fit theoretical predictions, subtracting it from the conductivity to find the interband contri-

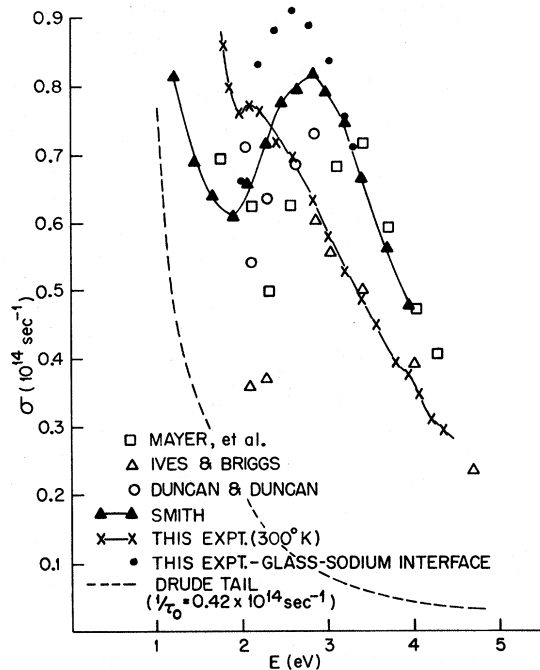


FIG. 12. Optical conductivity of sodium compared with previous experiments.

bution is a questionable procedure at this time. However, if the Drude tail is extrapolated into the interband region with the form  $\omega^{-2}$ , and the Butcher-Wilson expression<sup>2,3</sup> is used for the interband contribution, then the value  $|V_{110}| = 0.23$  eV obtained by Lee<sup>53</sup> from de Haas-van Alphen measurements best fits the data.

The results of this experiment closely agree with those of Ives and Briggs, who also used a vacuum interface. The two points in their data near 2.2 eV must be in error. Smith qualitatively disagrees with our data and with Ives and Briggs's data, but he qualitatively agrees with Duncan and Duncan, who also had a quartz-metal interface. In addition, we performed two independent measurements on a glass-sodium interface, and it can be seen from Fig. 12 that they agree qualitatively with Smith's results. This demonstrates that the presence of a dielectric at the reflecting surface influences the experimental results, in a manner which is not yet clear.

It appears that the quartz dielectric does more to the boundary conditions than merely change the dielectric constant at the interface. The presence of a quartz substrate will affect the surface roughness, and if the surface roughness is of the order of 100 Å, the roughness will account for one-third of the effective depth (skin depth) of the metal with regard to its optical properties. This alone could significantly affect the boundary conditions determining the optical properties. Unfortunately, very

little theoretical work has been done on this matter because of the difficulty of including surface roughness effects in calculations of the optical properties of finite conductivity metals.<sup>54</sup> However, it is evident from the above results that the effects of a surface dielectric should be considered in some detail.

#### VI. ENERGY-LOSS FUNCTION OF POTASSIUM

The energy-loss function  $-\text{Im}\epsilon^{-1}$  describes the ability of the electron gas to absorb energy.<sup>55</sup> The primary means of absorption for small wave vectors is the excitation of bulk plasmons, and the energy-loss function peaks sharply at  $\omega_p$ . The energy-loss function for potassium has been calculated and is shown in Fig. 13. The width of the peak is given by Eq. (10) with  $\omega = \omega_p$ . The plasma frequency is 3.8 eV and  $\epsilon_2(\omega_p) = 0.07$ , so that  $1/\tau_d = 0.26$  eV. The measured width of the energy-loss function is  $0.25 \pm 0.02$  eV.

#### VII. TABULATION OF OPTICAL CONSTANTS OF SODIUM AND POTASSIUM

Tables II and III list the results of our measurements of the optical constants of sodium and potassium. The data have been analyzed at periodic intervals in wavelength from the raw data, which are scanned continuously in wavelength. The tabulated values are for samples at room temperature; the structure arising from the excitation of surface plasmons is, therefore, absent for these annealed films.

#### VIII. CONCLUDING REMARKS

The purpose of this experiment was to help clarify the confusing state of the experimental determination of the optical constants of sodium and

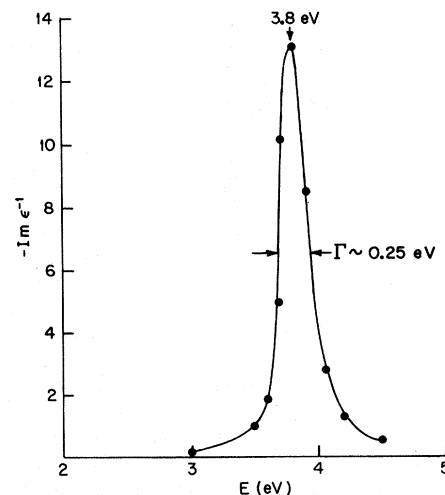


FIG. 13. Energy-loss function  $-\text{Im}\epsilon^{-1}$  for potassium.

TABLE II. Optical constants of sodium.

Energy (eV)	$\epsilon_1$	$\epsilon_2$	$\sigma$ ( $10^{14} \text{ sec}^{-1}$ )
1.79	-10.47	0.399	0.861
1.89	-9.03	0.347	0.794
1.95	-8.36	0.324	0.764
2.12	-6.93	0.302	0.774
2.23	-6.09	0.284	0.768
2.41	-4.97	0.247	0.720
2.61	-4.02	0.220	0.695
2.85	-3.14	0.183	0.632
3.06	-2.57	0.156	0.579
3.22	-2.18	0.138	0.537
3.40	-1.79	0.119	0.492
3.59	-1.49	0.104	0.453
3.82	-1.14	0.0855	0.395
3.94	-1.02	0.0788	0.375
4.07	-0.892	0.0707	0.348
4.20	-0.739	0.0611	0.310
4.35	-0.632	0.0560	0.295

TABLE III. Optical constants of potassium.

Energy (eV)	$\epsilon_1$	$\epsilon_2$	$\sigma$ ( $10^{14} \text{ sec}^{-1}$ )
1.76	-4.57	0.207	0.440
1.79	-4.38	0.209	0.451
2.02	-3.30	0.177	0.432
2.19	-2.63	0.152	0.405
2.41	-1.94	0.128	0.371
2.61	-1.45	0.115	0.362
2.79	-1.13	0.107	0.360
3.06	-0.728	0.0952	0.353
3.22	-0.552	0.0861	0.335
3.40	-0.344	0.0753	0.309
3.49	-0.268	0.0750	0.317
3.59	-0.184	0.0732	0.318
3.70	-0.0963	0.0708	0.317
3.82	-0.0185	0.0716	0.330
3.94	0.0574	0.0709	0.338
4.07	0.142	0.0678	0.333
4.20	0.212	0.0651	0.331
4.51	0.345	0.0633	0.346

potassium. The real part of the dielectric constant has been found to be well behaved, and its experimental values are taken to be reliable. Inconsistencies still remain in the measurement of the optical conductivity, however, despite vastly improved experimental techniques. This points out the historic difficulty in preparing alkali-metal films. However, we note that, as in the case of Smith, no evidence was found for the existence of the "Mayer-el Naby bump." One sample of potassium did exhibit an absorption peak at 1.5 eV, but since this particular sample was prepared differently (it was evaporated at a slower rate) and appeared grainy, we believe that this peak was produced by unusual surface structure and was not an intrinsic property of the metal.

Surface plasmons are readily producible on vac-

uum-interface films made at 77°K. Since the excitation of these modes couples to light through surface roughness, investigation of the behavior of surface plasmons under varying experimental conditions should prove invaluable not only to the resolution of the difficulties associated with determining the optical conductivity of the alkali metals, but also to the study of the physical properties of metal surfaces themselves.

#### ACKNOWLEDGMENTS

The authors would like to express their deep gratitude to Professor T. Carver, Professor J. Hopfield, and Professor J. Dow for their helpful comments. The work of S. Sari and Dr. A. Callender was invaluable to our efforts.

†Work supported by the National Science Foundation and the Westinghouse Electric Co.

\*National Science Foundation Predoctoral Fellowship.

‡A. P. Sloan Foundation Fellowship.

<sup>1</sup>M. H. Cohen, *Phil. Mag.* **3**, 762 (1958).

<sup>2</sup>P. N. Butcher, *Proc. Phys. Soc. (London)* **A64**, 50 (1951).

<sup>3</sup>A. H. Wilson, in *The Theory of Metals* (Cambridge U. P., New York, 1936), p. 133.

<sup>4</sup>J. A. Appelbaum, *Phys. Rev.* **144**, 435 (1966).

<sup>5</sup>A. O. E. Animalu, *Phys. Rev.* **163**, 557 (1967).

<sup>6</sup>H. E. Ives and H. B. Briggs, *J. Opt. Soc. Am.* **26**, 238 (1936).

<sup>7</sup>H. E. Ives and H. B. Briggs, *J. Opt. Soc. Am.* **27**, 181 (1937).

<sup>8</sup>R. W. Duncan and R. C. Duncan, *Phys. Rev.* **1**, 294 (1913).

<sup>9</sup>J. N. Hodgson, *J. Phys. Chem. Solids* **24**, 1213 (1963).

<sup>10</sup>J. N. Hodgson, *Phys. Letters* **7**, 300 (1963).

<sup>11</sup>H. Mayer and M. H. el Naby, *Z. Physik* **174**, 289 (1963).

<sup>12</sup>H. Mayer and B. Hietel, in *Proceedings of the International Colloquium on Optical Properties and Electronic Structure of Metals and Alloys* (North-Holland, Amsterdam, 1966), p. 47.

<sup>13</sup>R. Althoff and J. H. Hertz, *Infrared Phys.* **7**, 11 (1967).

<sup>14</sup>J. C. Sutherland, E. T. Arakawa, and R. N. Hamm, *J. Opt. Soc. Am.* **57**, 645 (1967).

<sup>15</sup>J. C. Sutherland and E. T. Arakawa, *J. Opt. Soc. Am.* **58**, 1080 (1968).

<sup>16</sup>N. V. Smith, *Phys. Rev.* **183**, 634 (1969).

<sup>17</sup>S. Jaspersen and S. Schnatterly, *Rev. Sci. Instr.* **40**, 761 (1969).

<sup>18</sup>A. B. Callender, Ph. D. dissertation (Princeton University, 1970) (unpublished).

<sup>19</sup>T. Holstein, *Phys. Rev.* **88**, 1427 (1952).

<sup>20</sup>R. B. Dingle, *Physica* **19**, 729 (1953).

<sup>21</sup>The ampoules containing 99.99% pure metal were

- purchased from Atomergic Chemetals Co., Carle Place, N. Y.
- <sup>22</sup>R. S. Sennet and G. D. Scott, *J. Opt. Soc. Am.* **40**, 203 (1950).
- <sup>23</sup>G. Hass, *J. Opt. Soc. Am.* **45**, 945 (1955).
- <sup>24</sup>D. Pines, in *Elementary Excitations in Solids* (Benjamin, New York, 1964), p. 144.
- <sup>25</sup>R. H. Ritchie, *Phys. Rev.* **106**, 874 (1957).
- <sup>26</sup>R. A. Ferrell, *Phys. Rev.* **111**, 1215 (1958).
- <sup>27</sup>E. A. Stern and R. A. Ferrel, *Phys. Rev.* **120**, 130 (1960).
- <sup>28</sup>C. J. Powell and J. B. Swan, *Phys. Rev.* **115**, 869 (1959); **116**, 81 (1959); **118**, 640 (1960).
- <sup>29</sup>H. Boersch, P. Dobberstein, D. Fritzsche, and G. Sauerbrey, *Z. Physik* **187**, 97 (1965).
- <sup>30</sup>H. Boersch and G. Sauerbrey, in Ref. 12, p. 386.
- <sup>31</sup>P. Von Blanckenhagen, H. Boersch, D. Fritzsche, H. G. Seifert, and G. Sauerbrey, *Phys. Letters* **11**, 296 (1964).
- <sup>32</sup>G. E. Jones, L. S. Cram, and E. T. Arakawa, *Phys. Rev.* **147**, 515 (1966).
- <sup>33</sup>E. T. Arakawa, R. N. Hamm, W. F. Hansen, and T. M. Jelinek, in Ref. 12, p. 374.
- <sup>34</sup>S. E. Schnatterly and S. N. Jasperson, *Phys. Rev.* **188**, 759 (1969).
- <sup>35</sup>O. Hunderi and D. Beaglehole, *Opt. Commun.* **1**, 101 (1969).
- <sup>36</sup>O. Hunderi and D. Beaglehole, *Phys. Letters* **29a**, 335 (1969).
- <sup>37</sup>D. Beaglehole and O. Hunderi, *Phys. Rev. B* **2**, 309 (1970).
- <sup>38</sup>O. Hunderi and D. Beaglehole, *Phys. Rev. B* **2**, 321 (1970).
- <sup>39</sup>Y.-Y. Teng and E. A. Stern, *Phys. Rev. Letters* **19**, 511 (1967).
- <sup>40</sup>P. A. Fedders, *Phys. Rev.* **165**, 580 (1968).
- <sup>41</sup>J. N. Mundy, L. W. Barr, and F. A. Smith, *Phil. Mag.* **15**, 411 (1967).
- <sup>42</sup>N. H. Nachtrieb, E. Catalano, and J. A. Weil, *J. Chem. Phys.* **20**, 1185 (1952).
- <sup>43</sup>R. A. Ferrel and E. A. Stern, *Am. J. Phys.* **30**, 810 (1962).
- <sup>44</sup>J. J. Hopfield, *Phys. Rev.* **139**, A419 (1965).
- <sup>45</sup>J. N. Hodgson, in Ref. 12, p. 60.
- <sup>46</sup>H. Ehrenreich and H. R. Phillip, *Phys. Rev.* **128**, 1622 (1962).
- <sup>47</sup>H. Ehrenreich, H. R. Phillip, and B. Segall, *Phys. Rev.* **132**, 1918 (1963).
- <sup>48</sup>H. E. Bennett and J. M. Bennett, in Ref. 12, p. 175.
- <sup>49</sup>H. E. Bennett and J. O. Porteus, *J. Opt. Soc. Am.* **51**, 123 (1961).
- <sup>50</sup>R. E. Palmer, Ph. D. dissertation (Princeton University, 1971) (unpublished).
- <sup>51</sup>R. N. Gurzhi, *Zh. Eksperim. i Teor. Fiz.* **35**, 965 (1958) [*Soviet Phys. JETP* **8**, 673 (1959)].
- <sup>52</sup>K. L. Kliewer and R. Fuchs, *Phys. Rev.* **172**, 607 (1968).
- <sup>53</sup>M. J. G. Lee, *Proc. Roy. Soc. (London)* **295A**, 440 (1966).
- <sup>54</sup>P. Beckmann and A. Spizzichino, in *Scattering of Electromagnetic Waves from Rough Surfaces* (Pergamon, New York, 1963), pp. 67-69, 97, and 98.
- <sup>55</sup>D. Pines, in Ref. 24, p. 151.

## Indium Diffusion in Aluminum

G. M. Hood and R. J. Schultz

*Atomic Energy of Canada Limited, Chalk River Nuclear Laboratories,  
Chalk River, Ontario, Canada*

(Received 22 March 1971)

Six measurements of  $^{114}\text{In}$  diffusion in single crystals of 99.999% pure Al have been made in the range 440-660°C. A least-mean-squares analysis of the data leads to the expression  $D = 1.16e^{-1.27eV/kT}$  cm<sup>2</sup>sec<sup>-1</sup>. The activation energy is similar to that found for the diffusion of other nontransition solutes in Al and does not therefore appear to reflect an exceptionally large In-vacancy binding energy in Al, such as was found by quenching experiments.

The choice of In for the present study was dictated largely by consistent reports of a relatively large binding energy between vacancies and In atoms in Al.<sup>1,2</sup> (Further references are listed in Ref. 1.)

It is expected, on general grounds, that a large solute-vacancy binding energy will be reflected in the difference between the activation energies  $\Delta Q$  for diffusion of the solute ( $Q_i$ ) and for self-diffusion ( $Q_0$ ) in a given solvent.<sup>3</sup>

In the present work, single crystals of 99.999% pure Al were used. Disks, 1 cm diam by 5 mm thick, were prepared metallographically and annealed under vacuum for 24 h at 620°C. They

were then implanted with 40-keV  $^{114}\text{In}$  ions in the CRNL mass separator. The advantages of this technique as a means of forming source layers for diffusion experiments are discussed elsewhere.<sup>4,5</sup> Diffusion anneals were carried out under vacuum. The samples were subsequently sectioned and analyzed for  $^{114}\text{In}$  by  $\gamma$ -ray counting techniques. Details of the sample preparation, sectioning, and counting techniques are described in Refs. 4 and 5.

The results are presented in Fig. 1 and Table I. Gaussian profiles were found for all samples, although an anomalous "wobble" appeared in the first few sections of each sample. For clarity this has been omitted; however, the insert in Fig.